J Solid State Electrochem (2007) 11:757–762
DOI 10.1007/s10008-006-0223-y

ORIGINAL PAPER

A new flow-type cell by the application of magnetic microfluidic chip

Ryoichi Aogaki · Eiko Ito · Mikio Ogata

Received: 14 April 2006 / Accepted: 29 August 2006 / Published online: 4 November 2006
© Springer-Verlag 2006

Abstract Using a magnetically formed channel called a magnetic channel, a new flow-type cell is proposed. The magnetic channel consists of magnetic walls that are formed by heterogeneous distributions of magnetic flux density around a ferromagnetic track under a magnetic field. The magnetic wall separates the paramagnetic oxidant solution from the diamagnetic reductant solution at a liquid–liquid interface without any solid membranes. In the magnetic channel formed on the cathode, the oxidant solution flows in a quasi-frictionless mode. The anode is placed in the reductant solution surrounding the magnetic channel. Such a geometrical configuration between the oxidant and reductant solutions is interchangeable depending on the magnetism of the solutions. To examine this concept, a Daniel cell system was adopted, where the copper ion in copper sulfate solution is employed as the oxidant and the zinc atom of zinc electrode as the reductant. The copper ion is paramagnetic, so that 1 mol dm^{-3} copper sulfate solution is injected into the magnetic channel formed on the copper cathode. Zinc sulfate solution (1 mol dm^{-3}; diamagnetic) together with the zinc anode are placed surrounding the magnetic channel. The performance of this flow-type battery was examined up to a current density of 22 mA cm^{-2}.

This paper was presented at the International Symposium on Magneto-Science 2005, Yokohama, 2005.

Contribution to the special issue "Magnetic Field Effects in Electrochemistry."

R. Aogaki (✉) · E. Ito · M. Ogata
Department of Electronic System Engineering,
Polytechnic University,
4-1-1, Hashimotodai, Sagamihara,
Kanagawa 229-1196, Japan
e-mail: aogaki@uitec.ac.jp

Keywords Magnetic field · Magnetic channel · Microfluidic chip · Fuel cell · Battery

Introduction

Recent social demand for developing new devices in the field of energy generation and storage has led many researchers to focus on developing various kinds of electrochemical cells.

As power sources, fuel cells and other flow-type cells have much similarity in continuously progressing electrochemical reactions; first, they have flow systems driven by pressure differences, which consist of solid channels separated by a static physical barrier for fuel and oxidant streams or oxidant and reductant streams. Currently, fuel cells designed with a proton exchanging membrane (PEM), which separates the fuel and oxidant in the anodic and cathodic compartments, are popular. Especially, direct oxidation-type fuel cells (DOFCs) using PEMs have significant advantages over reforming-type fuel cells in weight, volume, and simplicity of the system. The direct methanol fuel cell is a typical example of a DOFC. However, methanol crosses the PEM, such as Nafion, resulting in a lowered performance and fuel utilization efficiency [1]. Alternative organic fuels for the DOFC have been investigated to improve cell performance as well as fuel efficiency [2]. In spite of their favorable features, PEM-type cells still have some problems other than fuel crossover through the membranes, high-temperature operation for faster kinetics, and water management for proton transfer.

In a recent paper, a novel microfluidic fuel cell without a static physical barrier has been proposed; multi-stream laminar flow at the microscale keeps the fuel and oxidant

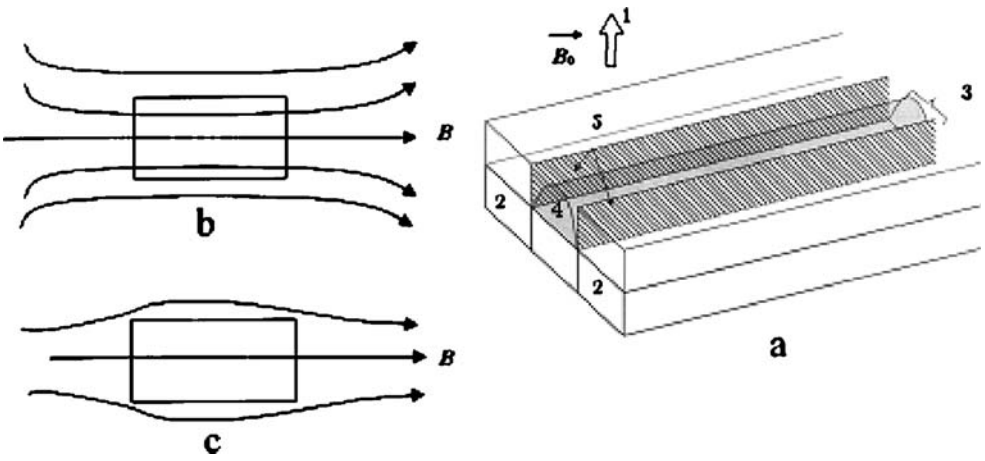

Fig. 1 Formation of the magnetic channel. **a** Schematics of magnetic walls for a diamagnetic solution surrounded by a paramagnetic solution. *1* Magnetic flux density; *2* ferromagnetic material; *3* diamagnetic material; *4* diamagnetic solution; *5* magnetic wall (*invisible*). **b** Distribution of magnetic flux density around a ferromagnetic material. **c** Distribution of magnetic flux density around a diamagnetic material

streams separated in diffusional contact. In this system, mass transfer proceeds across a mutual liquid–liquid interface without any solid membranes, which essentially requires laminar flows without turbulence [3]. Utilization of microfluidic systems with microchannels has resulted in a number of interesting applications, such as DNA chips [4], multiple biochemical analysis [5], and in-channel microfabrication [6]. The fluid flow is pressure-driven in a narrow solid channel, so that the formation of bubbles and particles would hinder the performance of the systems by disturbing the flows or, at worst, by choking up the channels. At the same time, due to the small cross-sectional area of the microchannel, a problem also arises that the area of the liquid–liquid interface is too small to obtain sufficient electric power.

The specific power source studied in the present paper, following the newly developed concept of magnetic microfluidic chips [7, 8], is a flow-type cell that utilizes a unique property of liquid flow at the microscale. Figure 1 schematically shows a microchannel for a liquid flow confined by magnetic walls that are generated by a heterogeneous magnetic field induced by a ferromagnetic track embedded on a substrate. To confine a solution of interest to a magnetic channel, a pair of liquids with weaker and stronger magnetisms, such as diamagnetism and paramagnetism, is necessary; one is called the test solution in the magnetic channel, and the other is called the environmental solution surrounding the magnetic channel. In the magnetic channel, the test solution flows in a quasi-inviscid mode so that a quite high liquid velocity is attainable. At the same time, even in a channel with 1-mm diameter (apparent Reynolds number $Re \approx 1$), small vortexes can be observed [7, 8], which are effective to decrease the diffusion layer thickness at the electrode. A liquid–liquid interface sepa-

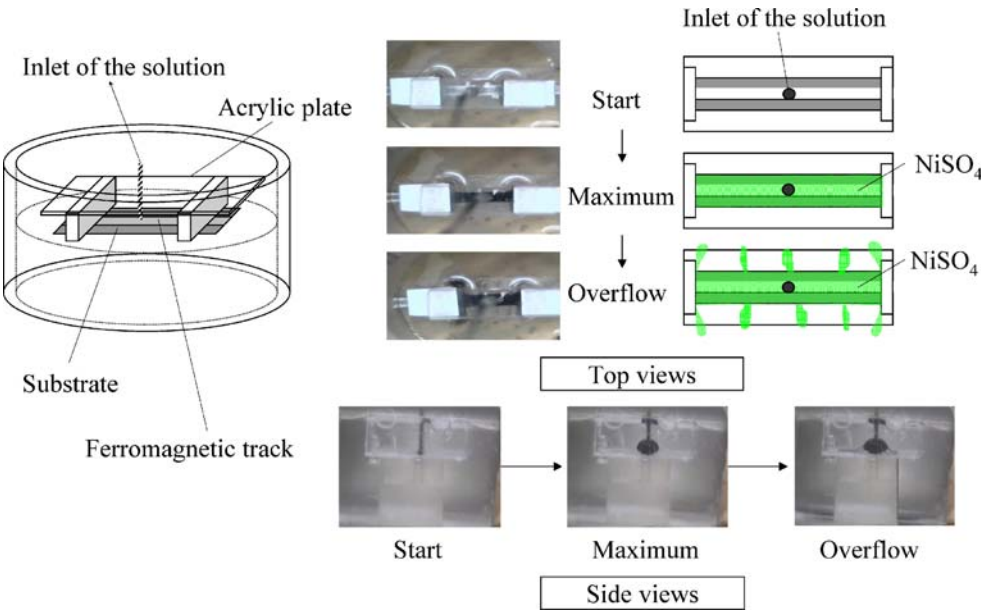

Fig. 2 Flexibility and reformability of magnetic channel. 1.4 mol dm^{-3} $NiSO_4$ solution was injected through a needle of a syringe into a magnetic channel. An iron track (1 mm wide, 2 cm long, and 1 mm thick) was embedded on an acrylic plate, of which both sides are stopped by acrylic blocks. A magnetic field of 7 T was vertically applied to the track

rated by the magnetic wall, which is stable without mixing across the interface, transversed to the direction of flow.

The other merits of the magnetic channel are its flexibility and self-reformability. As shown in Fig. 2, although invisible, a magnetic channel is formed on an iron track embedded on a substrate. The channel is surrounded by the diamagnetic water. A paramagnetic nickel sulfate solution is injected into the channel. As the channel is gradually filled with the nickel sulfate solution, the diameter of the channel is expanded. Beyond the maximum point of the capacity, from many parts of the interface, we can see leakage of the nickel sulfate solution. However, after the leakage, the broken points are closed, and the channel is quickly recovered.

The concept of a magnetic-channel-flow-based redox cell discussed here is shown in Fig. 3; for a paramagnetic solution containing a cathodic active species, although invisible, magnetic channels are formed on platinum-plated iron tracks embedded in a plastic plate. A diamagnetic solution with an anodic active species as an environmental solution surrounds the magnetic channels. The tracks are also used as the cathode, whereas the anode is placed above the cathode. Such a geometrical configuration of cathode and anode is interchangeable to give a paramagnetic environmental solution and a diamagnetic test solution. Because the magnetic wall surrounds the test solution on all sides, the area of the liquid–liquid interface is much larger than that of a one-sided interface in the solid microchannel. As shown in Fig. 2, the magnetic wall also acts as an elastic membrane, so that disturbance of the flow by bubbles and solid particles can be avoided by automatically changing the cross-sectional area of the channel. Because breaking points of the magnetic wall are automatically recovered, they are easily expelled to the surrounding environmental solution.

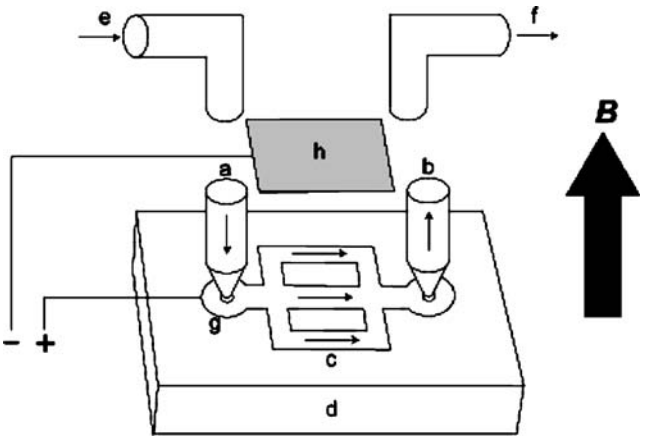

Fig. 3 Magnetic flow-type cell. **a** Inlet of cathodic active material; **b** its outlet; **c** magnetic channel (invisible); **d** plastic plate; **e** inlet of anodic active material; **f** its outlet; **g** cathode (Pt-plated iron track); **h** anode. *B* is the magnetic flux density

Theoretical

In general, there are two kinds of magnetic forces acting on a test solution confined by a magnetic channel [9]; one is a body force acting on a magnetic field, which is expressed by

$$\vec{f}_{\text{body}} = \frac{\Delta\chi}{\mu_0}\vec{B}\nabla\vec{B} \tag{1}$$

where μ_0 is the magnetic permeability, $\vec{B}$ is the magnetic flux density, and $\nabla\vec{B}$ is the gradient of $\vec{B}$. $\Delta\chi$ is the relative dimensionless magnetic susceptibility difference, where $\Delta\chi \equiv \chi_t - \chi_e$ is defined, and χ_t and χ_e are the dimensionless susceptibilities of the test and environmental solutions, respectively. Then, there is a surface force acting on the liquid–liquid interface at the magnetic wall, where there is a concentration gradient at the interface, so that the susceptibility gradient also generates a force, expressed as

$$\vec{f}_{\text{surf}} = \frac{1}{2\mu_0}\overrightarrow{B^2}\nabla\chi \tag{2}$$

By integrating Eq. 2 across the interface, a magnetic pressure per unit area of the interface is obtained [10], i.e.,

$$P_{\text{mag}} = \frac{\Delta\chi}{2\mu_0}\overrightarrow{B^2} \tag{3}$$

According to Coey et al. (to be published), the elastic-membrane-like quality of the interface in high magnetic fields (>1 T) is mainly due to the magnetic pressure in Eq. 3 instead of interfacial tension. Nearly frictionless, inviscid behavior of the test solution comes from the free boundary of the liquid–liquid interface of the magnetic channel. Therefore, characteristic features of the magnetic walls that are elastic and quasi-frictionless assure smooth streaming and stable interfaces.

In the present case, the Schmidt number $Sc = \nu/D$ (ν is the kinematic viscosity of the test solution, and D is the diffusion coefficient of the active species) is the ratio of momentum diffusivity to molecular diffusivity. In this case, the apparent Schmidt number is quite large (of order 10^4); however, it is actually treated as small because the magnetic channel flow seems frictionless. From the same point of view, the apparent Reynolds number $Re = Uh/\nu$ (U and h are the average velocity and channel height, respectively) is, as mentioned in "Introduction," very low (of order 1), corresponding to a completely laminar flow. However, it seems treated to be much higher, corresponding to a turbulent-like flow with vortexes, which reflects the instability at a fluid–fluid interface (the Kelvin–Helmholtz instability [11]). As the magnetic channel flow can be operated in high-speed mode, the effective Péclet number $Pe = Uh/D$ can be estimated to be of the order 10^4. Because the Péclet number indicates the ratio of diffusive

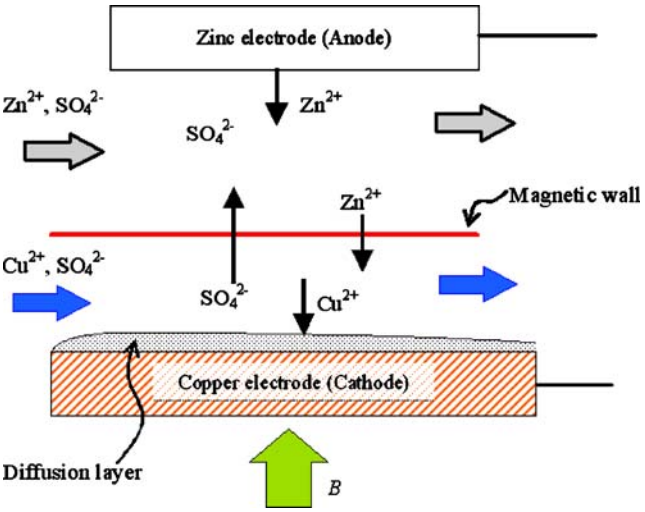

Fig. 4 Diffusion layer formation in the magnetic channel and ionic transfer across the magnetic wall

time to convective time in a stream, crossover through the magnetic channel is negligibly small.

Here, as a first step, instead of a fuel cell, a simple Daniel cell system and a permanent magnet were chosen to examine the characteristics of a magnetic-channel-flow-based cell. The Daniel cell involves the following reactions according to the half-cell notation:

$$Cu^{2+}(aq) + 2e^- \rightarrow Cu(s) \quad E^{\vartheta} = +0.34\,V \tag{4}$$

$$Zn^{2+}(aq) + 2e^- \rightarrow Zn(s) \quad E^{\vartheta} = -0.76\,V \tag{5}$$

where E^{ϑ} is the standard potential, and 'aq' and 's' mean aqueous and solid phases, respectively. The standard electromotive force is thus +1.10 V. As shown in Fig. 4, Zn^{2+} ions in the environmental solution can be prevented from crossing over if the test solution containing Cu^{2+} ions flows at high velocity. Such crossover also proceeds by the ionic migration of Zn^{2+} ions across the liquid–liquid interface, which is remedied by the addition of a large amount of supporting electrolyte. Owing to the turbulent-like flow, diffusion layer formation is disturbed, so that the thickness of the diffusion layer does not develop along the electrode, which is quite advantageous for mass transfer.

During the operation of the cell, a Lorentz force arises from the interaction between an electrolytic current and a magnetic field. The Lorentz force would induce a solution flow called magnetohydrodynamic (MHD) flow [12, 13]. However, owing to the small cross-sectional area of the magnetic channel, it is expected that the magnetic channel is hardly affected by the MHD flow, which rather helps mass transfer by convection.

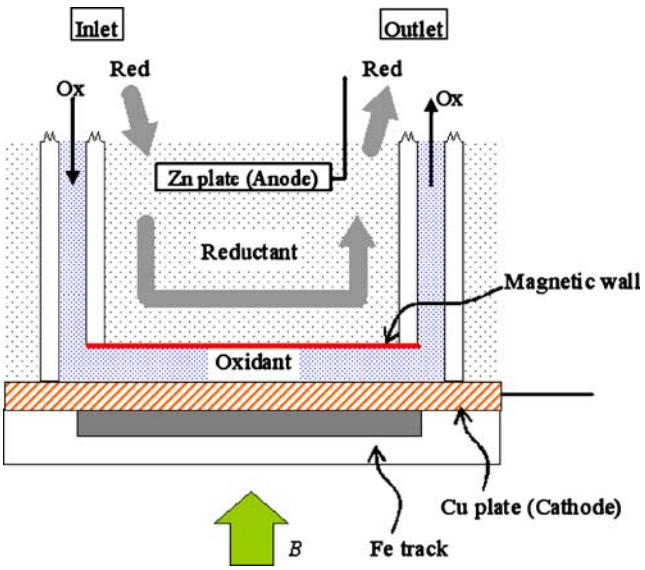

Fig. 5 Experimental setup of a magnetic flow-type cell

Experimental methods

$CuSO_4$ solution (1 mol dm^{-3}) and $ZnSO_4$ solution (1 mol dm^{-3}) were used as the cathodic active solution and the anodic active solutions, respectively. The paramagnetic copper sulfate solution was used as the test solution flowing in the magnetic channel. As shown in Fig. 5, the experimental setup of the flow-type cell consists of a straight iron track made of one or two iron wires (each is 4 cm long and 1 mm in diameter) embedded under the copper cathode (4 cm long, 4 mm wide, and 0.2 mm thick). The test solution was injected from the inlet, flowing through the magnetic channel to the outlet. The diamagnetic zinc sulfate solution was used as an ambient environmental solution, which was slowly circulated. Before the experiment, all the solutions were deaerated by a bubbling argon gas. A zinc plate (4 cm long, 5 mm wide, and 0.4 mm thick) was used as the anode. The copper cathode and zinc anode were mechanically polished just before the experiment. A beaker containing the cell and the environmental solution was placed in the 3-cm gap between the magnetic poles of a permanent magnet (the maximum magnetic flux density was 0.65 T, Kyoei Magnet Industry), i.e., a vertical magnetic field was employed. All experiments were conducted at room temperature. For the flow-

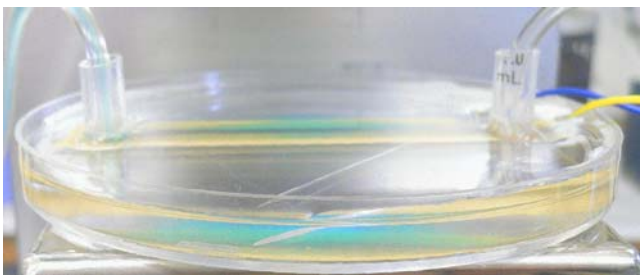

Fig. 6 Photo of magnetic microfluidic cell in operation

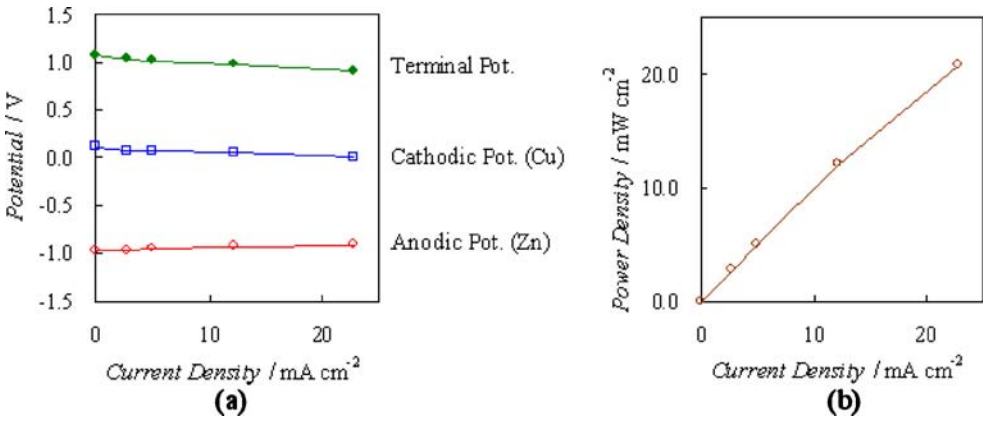

Fig. 7 Load curve and corresponding power density curve of magnetic microfluidic flow cell with 1 mol dm^{-3} $CuSO_4$ solution as the test solution and 1 mol dm^{-3} $ZnSO_4$ solution as the environmental solution. Flow velocity of the test solution is at 0.8 cm^3 min^{-1}. Embedded iron track is composed of a single iron wire 1 mm in diameter. **a** Load curve, **b** power density curve. *Terminal Pot.* denotes the terminal potential of cell

type cell characterization, the current and potential were measured at different loads (i.e., external resistances) using a variable resistor. Immediately after the experiment, to check the contamination from the crossover of zinc ions or copper ions, the potentials of the copper and zinc electrodes used in the cell were calibrated in 1 mol dm^{-3} copper sulfate solution and 1 mol dm^{-3} zinc sulfate solutions, respectively. Then, the electrode surfaces were observed by an optical microscope. As a result, zinc contamination on the copper electrode and copper contamination on the zinc electrode were not detected. Volume velocity of the flow was kept at 0.8 cm^3 min^{-1}. In Fig. 6, the actual experimental setup is shown; although invisible, the permanent magnetic poles are placed at the upper and lower sides of the flow-type cell.

Results and discussion

As shown in Figs. 7 and 8, load curves of the flow-type cells were obtained using 1 mol dm^{-3} copper sulfate solution and 1 mol dm^{-3} zinc sulfate. The terminal potentials at zero current (electromotive force) were equal to the theoretical value of 1.1 V. This can be ascribed to the fact that the contamination of zinc and copper ions on the electrodes was not detected. As discussed on the Péclet number, the result also represents that the crossover can be neglected. The iron track was made of one or two iron wires with a circular cross-section of 1-mm diameter. The active cathodic areas were measured by observing the copper deposition on the copper electrode surfaces with the optical microscope. In spite of the circular cross-section of the wire, the widths of the active area of the magnetic channel were approximately equal to 1 and 2 mm, corresponding to the number of iron wires. This characteristic feature implies that the magnetic channel does not depend on the three-dimensional shape of the iron track but on the projected shape onto the electrode surface. This point was ascertained by comparing the magnetic channel formed by the iron track with a 1-mm square cross-section, of which performance was approximately equal to that of the 1-mm diameter circular cross-sectional case.

In Figs. 7 and 8, the load curves of the two types of cells hardly decrease up to 20 mA cm^{-2}, whereas in the solid mirofluidic fuel cell [3], only at 8 mA cm^{-2}, the terminal potential decreases down to 10% of the initial value. This difference is attributed to the fact that the magnetic microfluidic cell has an inner cell resistance much lower than that of the solid microfluidic cell; although a simple configuration, the area resistance was about 7 Ω cm^2. In the

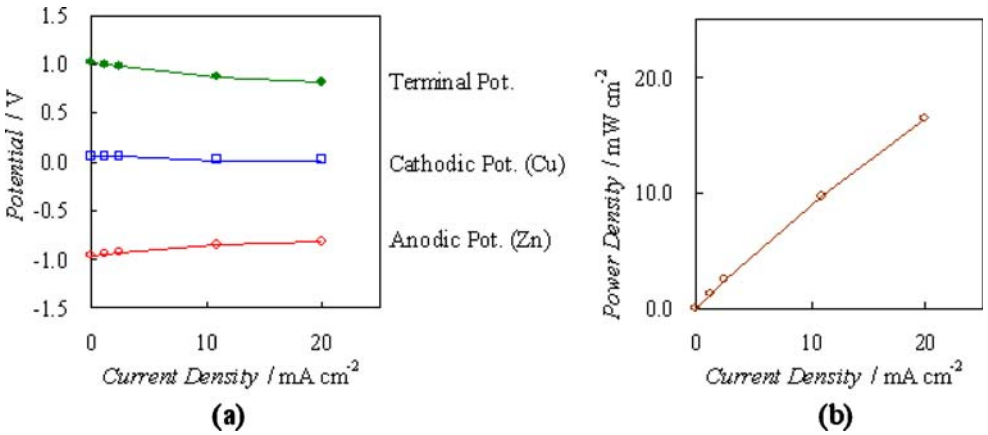

Fig. 8 Load curve and corresponding power density curve of the magnetic microfluidic flow cell with 1 mol dm^{-3} $CuSO_4$ solution as the test solution and 1 mol dm^{-3} $ZnSO_4$ solution as the environmental solution. Flow velocity of the test solution is 0.8 cm^3 min^{-1}. Embedded iron track is composed of two iron wires 1 mm in diameter. (**a**) Load curve, (**b**) Power density curve. *Terminal Pot.* denotes the terminal potential of the cell

case of the solid microfluidic fuel cell, the area resistance was 750 Ω cm^2. Such low inner resistance of the magnetic microfluidic cell comes from the large area of the liquid–liquid interface of the magnetic channel without solid walls and the vortex formation promoting mass transfer in the magnetic channel.

Corresponding power density curves of the magnetic microfluidic cell draw straight lines without optimal peaks up to 20 mW cm^{-2}. Both data for the two types of the iron track are similar to each other, which implies that the total power is proportional to the width of the magnetic channel, i.e., the width of the iron track. On the other hand, in the case of the solid microfluidic fuel cell, at about 4 mA cm^{-2}, the power density curve takes an optimal peak of 2.4 mW cm^{-2}. This difference is also attributed to the same reason as above. In addition, in the magnetic microfluidic cell, owing to the quasi-frictionless nature, it is easy to reform the performance with the increasing velocity of the magnetic channel flow.

Conclusions

The present prototype of a new flow-type cell is based on a simple Daniel cell, for which electrode areas were 0.4 and 0.8 cm^2, and achievable current densities were up to 22 mA cm^{-2}. This upper limit is modified by the increasing velocity of the magnetic channel flow owing to the quasi-frictionless flow property together with the low inner resistance without a solid membrane and a solid wall. The desired target is to design devices for more applicable redox flow cells or fuel cells. New designs will seek to exploit the characteristic advantages of the magnetic channel system. The current system possesses a flowing liquid membrane with high ionic conductance and high elasticity accompanied by the self-adjustable and self-reformable properties of the magnetic channel, which leads to the rapid removal of bubbles and solid particles, and precise control over the crossover of a particular component from the ambient solution phase. In the case of fuel cells, magnetic channels would remove solid membranes resulting in no water control for the maintenance of membranes and higher temperature tolerance. As for the permanent magnets, by designing more compact configurations of the channels, their size and weight can be minimized.

References

1. Wakabayashi N, Takeuchi K, Uchida H, Watanabe M (2004) J Electrochem Soc 151:A1636
2. Tucker MC, Odgaard M, Lund PB, Y-Andersen S, Thomas JO (2005) J Electrochem Soc 152:A1844
3. Choban ER, Markoski LT, Wieckowski A, Kenis PJA (2004) J Power Sources 128:54
4. Figeys D, Pinto D (2000) Anal Chem 72:330A
5. Roper MG, Shackman JG, Dahlgren GM, Kennedy RT (2003) Anal Chem 75:4711
6. Kenis PJA, Ismagilov RF, Whitesides GM (1999) Science 285:83
7. Aogaki R, Ito E, Ogata M (2003) Proceedings of the Symposium on New Magneto-Science 2003. Tsukuba, Japan, pp 70–76
8. Aogaki R, Ito E, Ogata M (2005) Proceedings of the Joint 15th Riga and 6th Pamir International Conference on Fundamental and Applied MHD, vol 1. Riga Jurmala, Latvia, pp 65–72, to be published in J. Magnetohydrodynamics
9. Sugiyama A, Hashiride M, Morimoto R, Nagai Y, Aogaki R (2004) Electrochim Acta 49:5115
10. Lahoz DG, Walker G (1975) J Phys D Appl Phys 8:1994
11. Chandrasekhar S (1981) Hydrodynamic and hydromagnetic stability. Dover, New York, pp 481–514
12. Aogaki R, Fueki K, Mukaibo T (1975) Denki Kagaku (presently Electrochemistry) 43:504
13. Aogaki R, Fueki K, Mukaibo T (1975) Denki Kagaku (presently Electrochemistry) 43:508